Inorganic Chemistry

Article

pubs.acs.org/IC

Reactions of Acids with Naphthyridine-Functionalized Ferrocenes: Protonation and Metal Extrusion

Nabanita Sadhukhan,[†] Mithun Sarkar,[†] Tapas Ghatak,[†] S. M. Wahidur Rahaman,[†] Leonard J. Barbour,[‡] and Jitendra K. Bera*[,†]

[†]Department of Chemistry, Indian Institute of Technology Kanpur, Kanpur 208016, India

[‡]Department of Chemistry, University of Stellenbosch, 7602, Stellenbosch, South Africa

Supporting Information

ABSTRACT: Reaction of 1,8-naphthyrid-2-yl-ferrocene (FcNP) with a variety of acids affords protonated salts at first, whereas longer reaction time leads to partial demetalation of FcNP resulting in a series of Fe complexes. The corresponding salts [FcNP·H][X] (X = BF_4 or CF_3SO_3 (**1**)) are isolated for HBF_4 and CF_3SO_3H. Reaction of FcNP with equimolar amount of CF_3CO_2H for 12 h affords a neutral complex [Fe(FcNP)$_2$(O_2CCF_3)$_2$(OH_2)$_2$] (**2**). Use of excess acid gave a trinuclear Fe^{II} complex [Fe_3(H_2O)$_2$(O_2CCF_3)$_8$(FcNP·H)$_2$] (**3**). Three linear iron atoms are held together by four bridging trifluoroacetates and two aqua ligands in a symmetric fashion. Reaction with ethereal solution of HCl afforded [(FcNP·H)$_3$(Cl)][$FeCl_4$]$_2$ (**4**) irrespective of the amount of the acid used. Even the picric acid (HPic) led to metal extrusion giving rise to [Fe_2(Cl)$_2$(FcNP)$_2$(Pic)$_2$] (**5**) when crystallized from dichloromethane. Metal extrusion was also observed for CF_3SO_3H, but an analytically pure compound could not be isolated. The demetalation reaction proceeds with an initial proton attack to the distal nitrogen of the NP unit. Subsequently, coordination of the conjugate base to the electrophilic Fe facilitates the release of Cp rings from metal. The conjugate base plays an important role in the demetalation process and favors the isolation of the Fe complex as well. The 1,1′-bis(1,8-naphthyrid-2-yl)ferrocene ($FcNP_2$) does not undergo demetalation under identical conditions. Two NP units share one positive charge causing the Fe-Cp bonds weakened to an extent that is not sufficient for demetalation. X-ray structure of the monoprotonated $FcNP_2$ reveals a discrete dimer [($FcNP_2$·H)]$_2$[OTf]$_2$ (**6**) supported by two N−H···N hydrogen bonds. Crystal packing and dispersive forces associated with intra- and intermolecular $\pi-\pi$ stacking interactions (NP···NP and Cp···NP) allow the formation of the dimer in the solid-state. The protonation and demetalation reactions of FcNP and $FcNP_2$ with a variety of acids are reported.

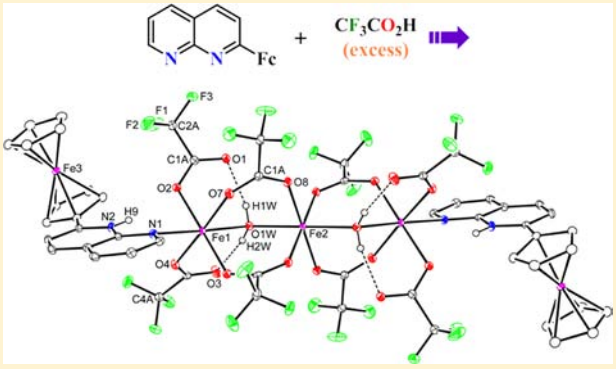

INTRODUCTION

Protonation of ferrocene (Fc), the simplest model for the electrophilic substitution of metallocene, has been the subject of numerous experimental and computational investigations.[1] The proton affinity of ferrocene is well recognized, but the precise site of proton attack remains an unresolved issue. NMR studies of Fc in aqueous BF_3 suggested a metal-hydride species in solution.[2] Subsequent experiments indicated a mixture of metal-protonated, agostic (endo), and ring-protonated (exo) species in deuterated medium (Scheme 1).[3] It has been proposed that the hardness of an electrophile determines the site of attack. A hard electrophile like acetyl cation (CH_3CO^+) prefers the ring-attack (exo) whereas mercuration by soft Hg^{2+} follows the metal-attack (endo).[4] For proton, a rapid equilibrium between metal-protonated and agostic forms is observed.[5] Thus, a clear preference for metal or ring-attack could not be established from the experimental data. Computational studies have afforded a set of contradicting conclusions. At the HF level, ring-protonation is favored over metal-protonation. Inclusion of electron correlation at the MP2 level, however, caused a reversal in the preferred site.[6] Calculations at CCSD(T) level of theory affords minima for metal-protonated

Scheme 1. Metal-Protonated (a), Agostic (b), and Ring-Protonated (c) Forms of Protonated Ferrocene

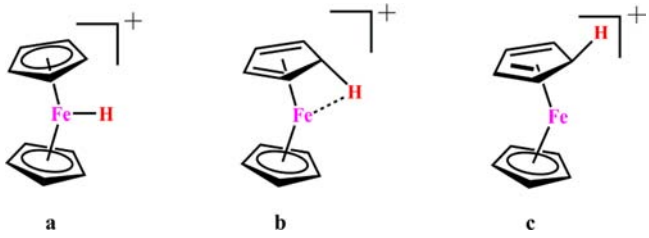

Received: October 3, 2012
Published: January 24, 2013

   dx.doi.org/10.1021/ic302155e | *Inorg. Chem.* 2013, 52, 1432−1442

and agostic forms, though no energy-minima structure was identified for ring-protonated form.[7]

Interaction of Li^+ with ferrocene revealed a stable structure where Li^+ was located on top of the π-face of the Cp ring.[8a,b] A lateral bound Li^+ to the iron atom of the ferrocene has also been reported.[8c] The Ga^+ interacts with ferrocene on top of the Cp ring in a multidecker complex consisting of alternate Ga^+ and ferrocene.[8d]

Intramolecular protonation of Fe by NH is reported in a ferrocenophane with bridging guanidines.[9a] Protonation by oxoanion HSO_4^- is credited for the remarkable fluorescence enhancement of a ferrocene-based ion pair receptor cobound with Pb^{II} or Zn^{II}.[9b] Acylferrocene (FcCOR) and ferrocenyl ethers $[Fc(CH_2)_nOR]$ are protonated at the carbonyl oxygen and ether oxygen, respectively, providing stable protonated species.[10] Density functional theory (DFT) studies on protonated formylferrocene show that the oxygen protonated isomer is stable compared to ring or metal-protonated species.[11]

Metal-ion coordination to functionalized ferrocenes has produced a rich chemistry providing access to myriad of heterobimetallic complexes.[12] In general, the metal ion binds the donor atom of the ferrocene appendage. Careful examination has revealed additional interactions which are worth mentioning. A Ni−Fe heterobimetallic complex featuring Fe→Ni dative bond has been reported with ferrocenedithiolato ligand (Scheme 2a).[13a] Similarly, Fe···Zr,[13b] Fe···Pd,[13c,d]

Scheme 2. Heterobimetallic Complexes of Ferrocene Based Ligands Showing Fe···M and M···Cp Interactions

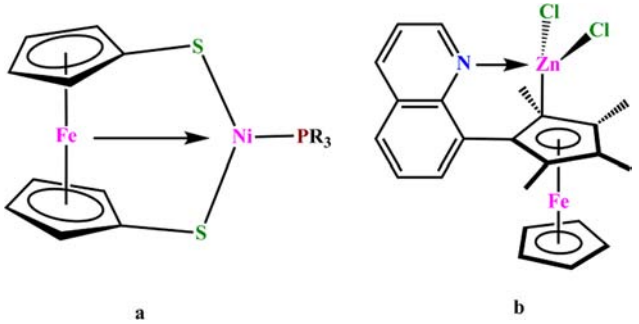

Fe···Zn,[13e] and Ru···Cu/Zn[13f] interactions are reported in complexes containing metallocene based ligands. Reaction of $ZnCl_2$ with 1,1′-bis(quinolyl)metallocene (Fc*Qu) afforded $[ZnCl_2(Fc*Qu)]$ which exhibits interaction of Zn with carbon atom of the Cp ring (Scheme 2b).[14]

Reductive degradation of ferrocene was reported long back by the application of Li in methylamine to metallic iron and cyclopentadiene.[15] Interaction of Lewis acid BCl_3 with the functionalized Cp ring in Fc*Qu led to Fe extrusion from the ligand affording an organoborane compound.[14] Molina and co-workers have reported metal extrusion from a bis-ferrocenyl-azaheterocycle on treatment with HBF_4 or HCl.[16] Herein, we disclose the protonation and metal extrusion of 1,8-naphthyrid-2-yl-ferrocene (FcNP) and 1,1′-bis(1,8-naphthyrid-2-yl)-ferrocene ($FcNP_2$) (Scheme 3) with a variety of acids.

RESULTS AND DISCUSSIONS

The coordination chemistry of naphthyridine-functionalized ferrocene derivatives FcNP and $FcNP_2$ is described in a recent report.[17] Reaction of $FcNP_2$ with Cu^I afforded a metallamacro-

Scheme 3. Line Drawings of FcNP and $FcNP_2$

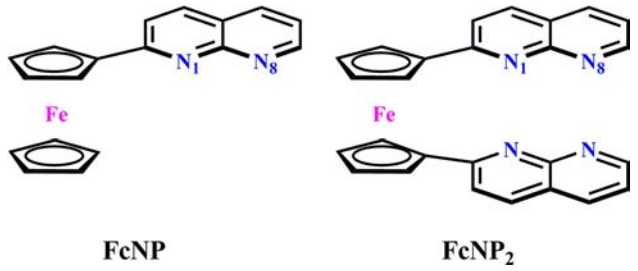

cycle comprising two head-on ligands bridged by two metal ions. A similar macrocycle supported by intermolecular hydrogen bonding (H-bonding) interactions is obtained upon protonation of $FcNP_2$. This initial result prompted us to explore other protonated ferrocene-naphthyridine hybrids which eventually lead to a wider investigation. While protonated salts were isolated for HBF_4 and CF_3SO_3H, partial release of metal from FcNP occurred upon reactions with CF_3COOH, HCl, and picric acid resulting in different Fe complexes containing the corresponding conjugate anions. $FcNP_2$ does not undergo demetalation under identical condition, and affords both mono- and bis-protonated adducts.

Protonation of FcNP. *Reactions with CF_3SO_3H and HBF_4.* Reaction of triflic acid to a methanolic solution of FcNP in 1:1 molar ratio for 1 h afforded a purple solid [FcNP·H][OTf] (**1**). Triflate anion is found to be H-bonded with the N−H hydrogen through one of the oxygen atoms (Supporting Information, Figure S1). The NP unit is planar with the Cp ring (inclination angle: ∠N2−C8−C9−C10 = 4.4(3)°). Reaction with HBF_4 provided an analogous protonated salt [FcNP·H]-[BF_4] which shows protonation at N_8 and its H-bonding interaction with one of the F atoms of BF_4^-.[18]

Reaction with Equimolar CF_3CO_2H. Reaction of CF_3CO_2H with FcNP in 1:1 molar ratio for 12 h afforded a neutral complex $[Fe(FcNP)_2(O_2CCF_3)_2(OH_2)_2]$ (**2**). The most remarkable feature of this complex is the central iron which originates from FcNP. The molecular structure reveals two FcNP, two trifluoroacetates, and two water molecules coordinated to Fe in mutually trans orientations creating an octahedral geometry around the metal (Figure 1). Each FcNP exhibits preferential κ^1-binding utilizing N_8 of the NP unit. The Fe1−N1 distance is 2.271(2) Å. The Fe1−O1W (aqua) distance is 2.132 (2) Å, and the Fe1−O2A (carboxylate) distance is 2.125 (2) Å. The cis angles are in the range 84.54(7)°−95.46(7)°.

Reaction with Excess CF_3CO_2H. Reaction of trifluoroacetic acid to a methanolic solution of FcNP in excess (10:1 molar ratio) for 12 h afforded a neutral, linear trinuclear Fe^{II} compound $[Fe_3(\mu\text{-}H_2O)_2(\mu\text{-}O_2CCF_3)_4(\kappa^1O\text{-}O_2CCF_3)_4(\kappa^1N_8\text{-}FcNP{\cdot}H)_2]$ (**3**) in high yield (70%). The molecular structure, as shown in Figure 2, consists of three iron atoms forming a linear array (∠Fe···Fe···Fe = 180°). The central iron resides on a crystallographically imposed inversion center. Three iron atoms are held together by four bridging trifluoroacetates and two bridging aqua ligands in a symmetric fashion. Each terminal iron is additionally coordinated to two monodentate trifluoroacetates. The trinuclear core is capped by protonated FcNP on both sides limiting the formation of a higher order oligomer. The distal nitrogen (N_8) in FcNP is utilized for metal coordination whereas the proximal nitrogen (N_1) is found to be protonated. Engagement of both N atoms of FcNP to metal

dx.doi.org/10.1021/ic302155e | Inorg. Chem. 2013, 52, 1432−1442

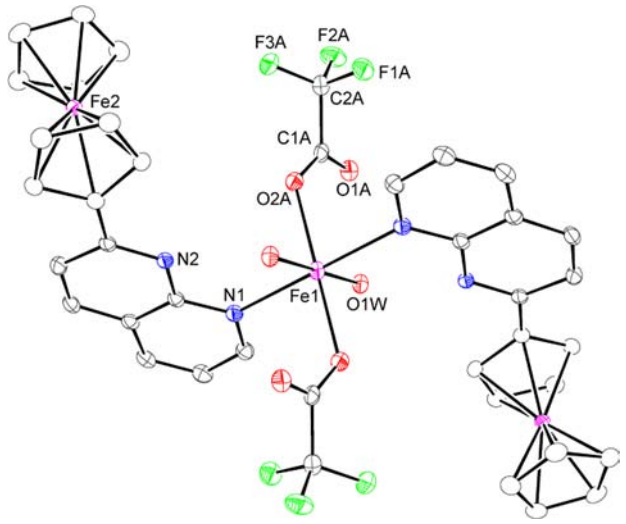

Figure 1. ORTEP diagram (40% probability thermal ellipsoids) of **2** with important atoms labeled. Carbon atoms of the ferrocene units are shown as circles of arbitrary radius. Hydrogen atoms are omitted for the sake of clarity. Selected bond distances (Å) and angles (deg): Fe1−O2A 2.125(2), Fe1−O1W 2.132(2), Fe1−N1 2.271(2), O1W−Fe1−O1W′ 180.00. Symmetry code: 1−*X*, 1−*Y*, −*Z*.

ions was reported earlier for dicopper(I) and dirhodium(II) complexes.[17a] The Fe···Fe separation is 3.726(1) Å. The Fe−O (carboxylate) distances are in the range 2.049(2)−2.119(2) Å. The Fe1−O1W distance is 2.239(2) Å, and the Fe1−O1W−Fe2 angle is 115.33(10)°. The unbound oxygen atoms of monodentate trifluoroacetates are engaged in H-bonding with the bridged water molecules. The OW−(H)···O distances are 2.644 and 2.687 Å. Each iron center possesses an octahedral geometry revealing a small range of deviation in cis (86.7(1)°−93.5(1)°) and trans (177.5(1)°−178.9(1)°) angles.

The spectroscopic and electrochemical data of the crude solid do not match with that of pure **3** indicating the existence of other products. It is possible that several oligomeric complexes are formed in solution. Neutral compound **3** separates out from the solution in form of crystals probably because of its lesser solubility.

Binuclear iron complexes bearing carboxylate ligands have attracted considerable attentions because of their relevance in nonheme iron enzymes.[19] The active site of one such enzyme, soluble methane monooxygenase (MMO) which converts methane to methanol by using O_2, contains a diiron core wrapped by four glutamate carboxylates and two histidine imidazoles (Scheme 4).[20] Metal-bound water molecules, further

Scheme 4. Active Site of Non-Heme Iron Enzyme

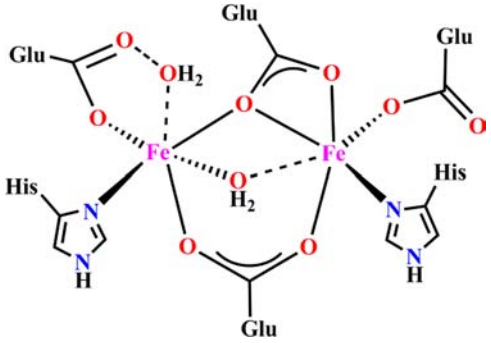

supported by H-bonding interactions with the carboxylates, are recognized to be the key components for oxygen binding and activation.[21] This led to a conscious effort for the synthesis of model complexes containing water molecules in the coordination sphere of diiron(II) carboxylate.[22] The triangular $\{Fe_3O(O_2CR)_6\}$ unit has dominated the chemistry of iron carboxylates for decades.[23] We are aware of an example $[Fe^{II}_3(\mu\text{-}O_2CCH_3)_6(\kappa^2\text{-biphme})_2]$[24] (biphme = 2,2′-(methoxy(phenyl)methylene)bis(1-methyl-1*H*-imidazole)) which contains a linear Fe_3 core supported by only the acetates (Fe···Fe = 3.3251(9) Å) (Scheme 5). Complex **3** is the only example of a linear trinuclear iron complex with bridging aqua and carboxylate ligands.

Reaction with HCl. Reaction of 1(M) HCl in Et_2O with FcNP (1:1 molar ratio) in methanol for 12 h afforded $[(FcNP{\cdot}H)_3(Cl)][FeCl_4]_2$ (**4**). The same product was isolated when excess acid (10-fold) was used. The asymmetric unit consists of three protonated $[FcNP{\cdot}H]^+$, one chloride, and two

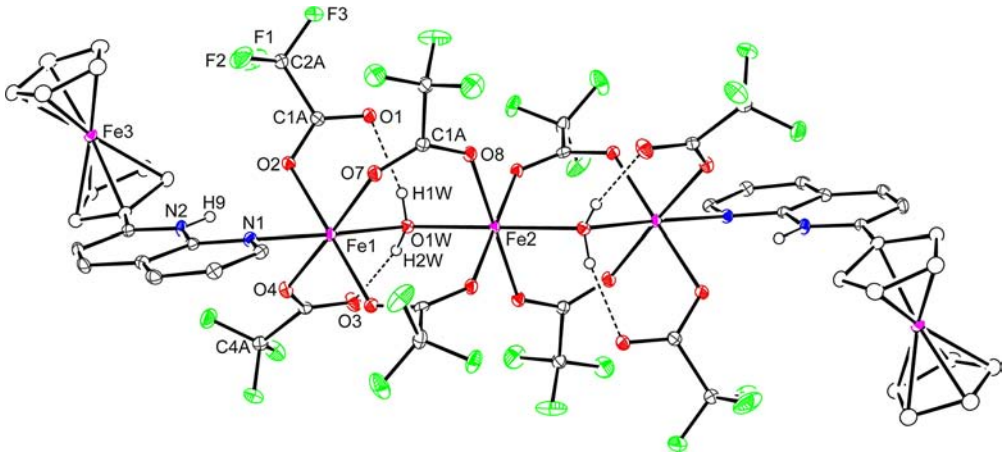

Figure 2. ORTEP diagram (40% probability thermal ellipsoids) of **3** with important atoms labeled. Carbon atoms of the ferrocene units are shown as circles of arbitrary radius. Hydrogen atoms except water and N−H are omitted for the sake of clarity. Selected bond distances (Å) and angles (deg): Fe1···Fe2 3.726(1), Fe1−O1W 2.239(2), Fe2−O1W 2.171(2), Fe1−N1 2.224(2), Fe1−O7 2.119(2), Fe1−O4 2.099(2), Fe1−O2 2.094(2), O1W−(H1W)···O1 2.687(3), O1W−(H2W)···O3 2.644(4). O4−Fe1−O1W 91.56(9), O5−Fe1−N1 91.40(9), O5−Fe1−O1W 90.61(9), O8−Fe2−O1W′ 91.71(8), Fe2−O1W−Fe1 115.33(10), O2−Fe1−O1W 90.48(8), Symmetry code: 1−*X*,−*Y*, 1−*Z*.

dx.doi.org/10.1021/ic302155e | *Inorg. Chem.* 2013, 52, 1432−1442

Scheme 5. Examples of Linear Trinuclear Fe(II) Complexes

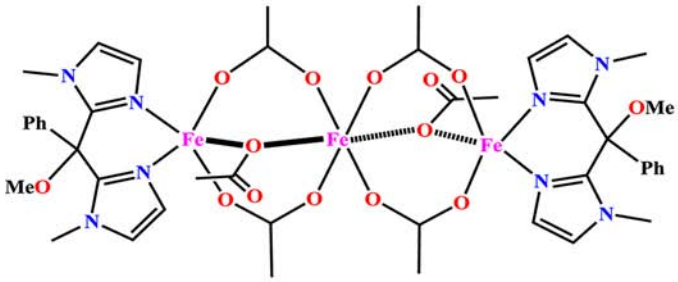

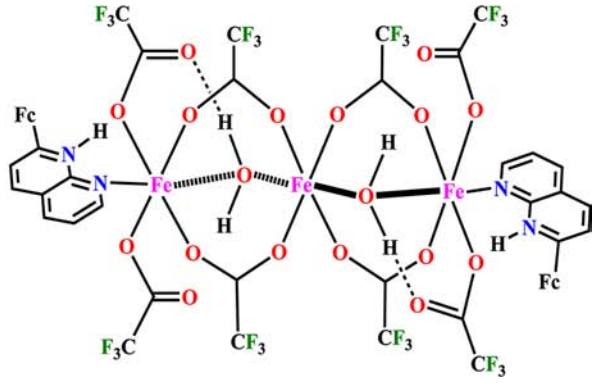

$[FeCl_4]^-$. X-ray structure reveals protonation at the N_8 atom of NP, and all three NH hydrogens are engaged in H-bonding interactions with the central chloride in pseudo C_3 symmetry (Supporting Information, Figure S2). As in previous cases, the source of iron in $[FeCl_4]^-$ is FcNP. It is likely that the bivalent iron that is extracted from ferrocene is oxidized to Fe^{III} by the adventitious oxygen.

Reaction with Picric Acid. Prompted by the metal extrusion from FcNP by certain acids, we wondered if the same could be achieved with an organic acid. Reaction of FcNP with 1 equiv of picric acid (HPic) in methanol for 12 h led to an immediate color change from orange red to green. Subsequent crystallization of the product from dichloromethane/petroleum ether afforded a neutral compound $[Fe_2(\mu\text{-}Cl)_2(FcNP)_2(Pic)_2]$ (**5**). Use of a mixture of acetonitrile/diethyl ether as crystallizing solvents afforded chloride-free neutral Fe(FcNP)-$(Pic)_2$ which was characterized spectroscopically.[25] This suggests that the source of chlorides in **5** is the dichloromethane employed during crystallization. We could not isolate a clean identifiable product when excess acid was used. The X-ray structure of **5** reveals partial demetalation resulting in a dinuclear Fe^{II} complex bridged by two chlorides. The origin of iron is FcNP as in previous cases. Complex **5** possesses a crystallographically imposed C_2 symmetry, and only half of the molecule is observed in the asymmetric unit (Figure 3). The geometry around each iron is pseudo octahedral consisting of one bidentate chelate picrate, one chelate FcNP, and two bridging chlorides. The Fe···Fe distance is 3.430(1) Å. The naphthyridine chelates the metal ion with bite angle 59.97(11)°.[26] The Fe−Cl distance and Fe−Cl−Fe angle are 2.4201(10) Å and 90.05(3)°, respectively. The picrate anion utilizes oxygen atoms of the phenoxy and one of the ortho-nitro groups to coordinate with the metal. Notable is the difference in Fe−O distances, the nitro oxygen makes longer Fe−O distance (2.226(2) Å) compared to phenoxy oxygen (1.982(2) Å). The cis (59.97(11)°−106.46(10)°) and trans angles (153.85(8)−174.45(7)°) reveal severe distortions from the ideal octahedral geometry around the central iron atom.

Transition metal-picrate complexes are relatively rare although picrates have been used widely in lanthanide chemistry.[27] A Cambridge Crystallographic Data Centre (CCDC) search revealed several complexes with group 11 metals Cu and Ag.[28] Examples of Mn^{II} complexes incorporating picrate ligands are known in the literature.[29] It appears that complex **5** is the only example of an iron complex containing picrate ligands mounted on a doubly chloro-bridged Fe_2Cl_2 core.

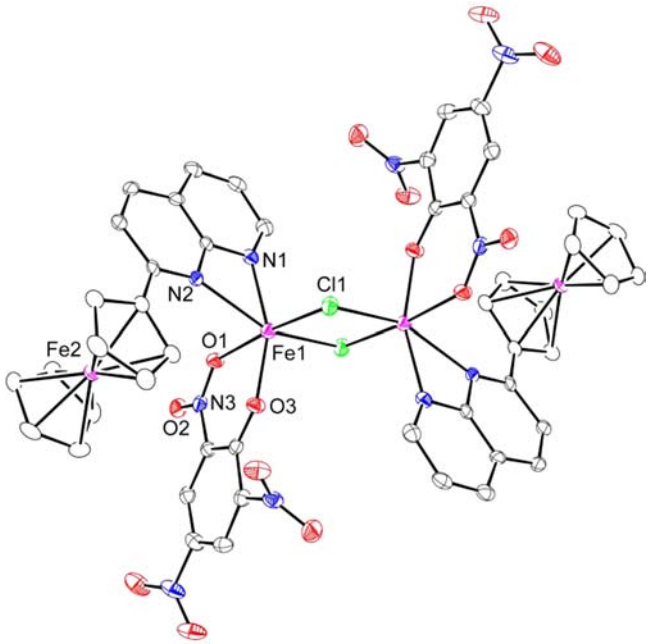

Figure 3. ORTEP diagram (50% probability thermal ellipsoids) of **5** with important atoms labeled. Carbon atoms of the ferrocene units are shown as circles of arbitrary radius. Hydrogen atoms are omitted for the sake of clarity. Selected bond distances (Å) and angles (deg): Fe1···Fe1′ 3.429 (1), Fe1−N1 2.129(3), Fe1−N2 2.368(3), Fe1−O1 2.226(2), Fe1−O3 1.982(2), Fe1−Cl1 2.420(10), Fe1−Cl1′ 2.432(1), Fe1−Cl1−Fe1′ 89.95(3), O3−Fe1−Cl1 95.60(7), N1−Fe1−Cl1 102.70(8), O3−Fe1−O1 78.99(10), N1−Fe1−N2 59.97(11), N2−Fe1−Cl1 94.36(7), Cl1−Fe1−Cl1′ 90.05(3). Symmetry code: 1−*X*, 1−*Y*, 1−*Z*.

Protonation of $FcNP_2$. Protonation of $FcNP_2$ with one or more equivalents of triflic acid afforded red-colored needle-shaped crystals of molecular formula $[(FcNP_2{\cdot}H)]_2[OTf]_2$ (**6**) in high yield. X-ray structure reveals a discrete H-bonded dimer reminiscent of $[Cu_2(FcNP_2)_2]^{2+}$ metallamacrocycle reported earlier by us.[17a] Molecular structure shows two $[FcNP_2{\cdot}H]^+$ units in head-on arrangement, linked by intermolecular N−H···N hydrogen bonds (Figure 4). Only half of the dimer was observed in the asymmetric unit related to the other half by a center of inversion. The N2···(H4)−N4 distance is 2.705(4) Å and N2−H4−N4 angle is 169.73(5)°. The rectangular shaped H-bonded dimer **6** features a box width of 11.366(1) Å (Fe···Fe separation) comparable to $[Cu_2(FcNP_2)_2]^{2+}$ (Fe···Fe = 11.104(3) Å).

dx.doi.org/10.1021/ic302155e | *Inorg. Chem.* 2013, 52, 1432−1442

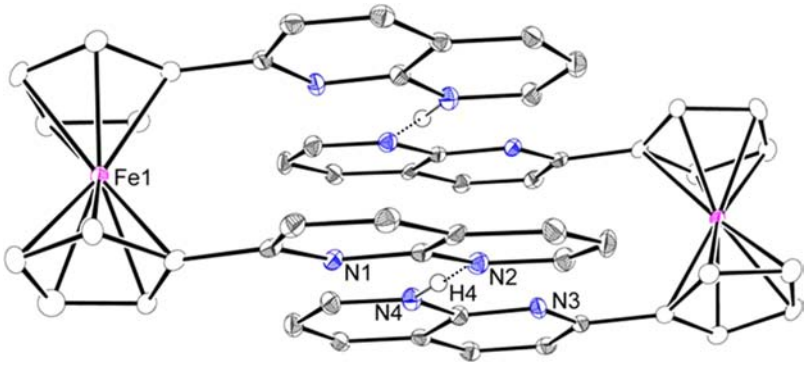

Figure 4. ORTEP diagram (40% probability thermal ellipsoids) of the dicationic unit $[(FcNP_2{\cdot}H)_2]^{2+}$ in **6** with important atoms labeled. Carbon atoms of the ferrocene units are shown as circles of arbitrary radius. Hydrogen atoms except N−H are omitted for the sake of clarity. Selected bond distances (Å) and angles (deg): N4−(H4)···N2 2.705(4). N4−H4−N2 169.73(5). Symmetry code: 1−*X*, −*Y*, −*Z*.

The NP units in free $FcNP_2$ are in a trans conformation.[17b] Protonation leads to 180° rotation along the C_5 axis resulting in a cis geometry stabilized through H-bonding interactions with the second molecule. Similar observation is reported for $[Fc(CO_2)_2]^{2-}$ which exhibits a trans conformation like $FcNP_2$. Protonation leads to a *syn* chelate geometry for $[Fc(CO_2)(CO_2H)]^-$ which acquire thermodynamic stability via H-bond interactions between $-CO_2^-$ and $-CO_2H$ units.[30]

The mother liquor obtained after isolation of **6** was kept in a refrigerator, and a small crop of crystals of different morphology (block-shaped) was harvested after 3 weeks. X-ray analysis confirmed it as the bis-protonated salts $[FcNP_2{\cdot}H_2][CF_3SO_3]_2$ (**7**). Molecular structure reveals protonation at the N_8 atom of both NP units. Further, the N−H hydrogens are engaged in H-bonding interactions with two independent triflates (Figure 5). The Cp and NP planes are planar and NP nitrogens are disposed in opposite directions. This is in sharp contrast to the NP arrangement in monoprotonated complex **6**. Precedence of a double protonated structure $[FcQu_2{\cdot}H_2]^{2+}$ ($FcQu_2$ = 1,1′-bis(8-quinolyl)ferrocene) exists in the literature.[13b]

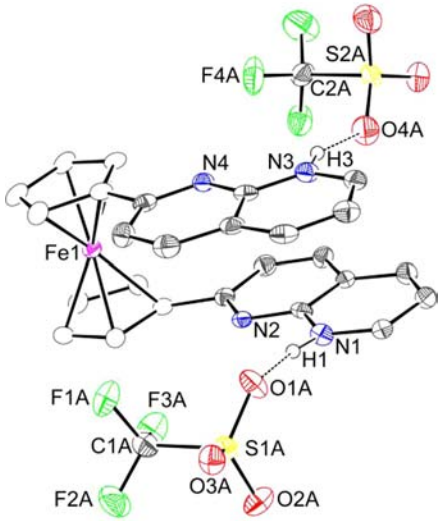

Figure 5. ORTEP diagram of (50% probability thermal ellipsoids) **7** with important atoms labeled. Carbon atoms of the ferrocene units are shown as circles of arbitrary radius. Hydrogen atoms except N−H are omitted for the sake of clarity. Selected bond distances (Å) and angles (deg): N1−(H1)···O1A 2.732(5), N3−(H3)···O4A 2.718(5) N1−H1−O1A 161.44(6), N3−H3−O4A 155.21(5).

Cyclic Voltammetry Studies. The electrochemical properties of compounds **1**−**6** are studied by cyclic voltammetry in propylene carbonate, and the redox potential values are collected in Table 1. Substitution of the Cp ring with a NP unit brings about a shift of 60 mV for ferrocenyl oxidation with respect to ferrocene ($E_{1/2}$ for Fc = 0.47(60) V under identical experimental conditions). The second substitution causes further positive shift of the oxidation by 130 mV. Modulation of redox potential by Cp ring substitution with pyridyl and pyrimidyl groups has been reported, and the values observed for naphthyridine derivatives are in close agreement.[31]

Table 1. Electrochemical Potentials (in Volt) from Cyclic Voltammetry for FcNP, $FcNP_2$, and 1−6 in Propylene Carbonate

compounds	oxidation	reduction
FcNP	0.53(180)[a]	−1.93[c]
$FcNP_2$	0.66(100)[a]	−1.87[c]
1	0.64(140)[a]	−1.59[c]
2	0.59(120)[a], 0.48[b]	−1.93[c]
3	0.57(70)[a], 0.15(170)[a]	−0.78[c]
4	0.64(120)[a]	−0.48[c], −1.66[c]
5	0.64(110)[a], 0.06(74)[a]	−1.89[c]
6	0.93(111)[a]	−0.49[c], −0.80[c]

[a]Half-wave potentials evaluated from cyclic voltammetry as $E_{1/2} = (E_{p,a} + E_{p,c})/2$, peak potential differences in mV in parentheses. [b]Peak potentials, $E_{p,a}$ for irreversible oxidation processes. [c]Peak potentials, $E_{p,c}$, for irreversible reduction processes.

Protonation causes an anodic shift of 110 mV of Fc^+/Fc couple with respect to FcNP reflecting a significant charge transfer from ferrocenyl donor to NP based acceptor. The NP based reduction appears at $E_{p,c}$ = −1.59 V indicating easier reduction of the protonated NP unit. Complex **2** exhibits ferrocenyl oxidation at $E_{1/2}$ = 0.59(120) V which is 50 mV lower than that of the protonated complex **1**. The irreversible oxidation of the central iron appears at $E_{p,a}$ = 0.48 V. Although complex **3** contains three different Fe-based moieties, namely, protonated FcNP, two terminal Fe, and a central Fe of the trinuclear core, only two oxidation processes at 0.15(170) V and 0.57(70) V are observed. Although the first oxidation can safely be assigned to the Fe_3 core, the same is not so obvious for the second oxidation. It is unlikely that the metal-coordinated $FcNP.H^+(N_1)$ would oxidize at such a low potential since the N_8 protonated ligand oxidizes at 0.64 V in

dx.doi.org/10.1021/ic302155e | *Inorg. Chem.* 2013, 52, 1432−1442

1. Simultaneous protonation at proximal nitrogen (N_1) and metal-coordination through N_8 should make the FcNP highly electron deficient, which is reflected in the low reduction potential at $E_{p,c} = -0.78$ V. Accordingly, we attribute both these oxidation processes to the Fe_3 core. The FcNP·H^+ in **3** does not appear to exhibit oxidation within the accessible range of this experiment. The Fc-based oxidation potential in **4** is identical to **1**. It is understandable since both complexes essentially contain the protonated FcNP. Complex **4** exhibits an irreversible reduction at $E_{p,c} = -0.48$ V which is attributed to the anionic $[Fe^{III}Cl_4]$ core. Two reversible oxidation processes are recorded for compound **5** at $E_{1/2} = 0.64(110)$ and 0.06(74) V which correspond to Fe^{III}/Fe^{II} couples for FcNP and Fe_2Cl_2 core, respectively (Figure 6). The ferrocene based oxidation in

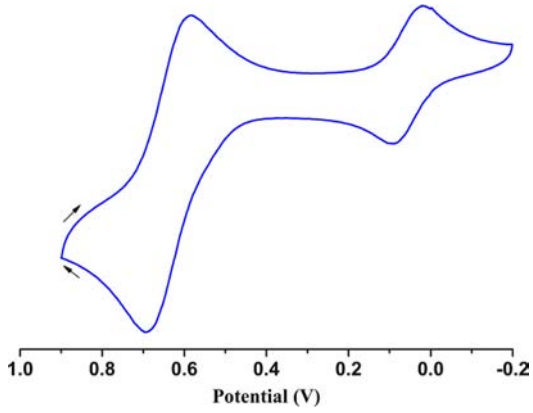

Figure 6. Cyclic voltammogram of **5** measured at scan rate of 100 mV/s in propylene carbonate.

6 appears at $E_{1/2} = 0.93(111)$ V which is 270 mV shifted toward positive potential with respect to $FcNP_2$. The reduction region consists of two irreversible waves at −0.49 and −0.80 V.

Electronic Spectroscopy. The electronic spectra of FcNP, $FcNP_2$, and compounds **1**−**6** were recorded in dichloromethane. The λ_{max} values with the corresponding log ε (ε = $dm^3\ mol^{-1}\ cm^{-1}$) values are collected in Table 2. The electronic

Table 2. Electronic Absorption Data for FcNP, $FcNP_2$, and Compounds 1−6 in Dichloromethane Solvent at Room Temperature

	absorption spectra
compounds	λ_{max}, nm (log ε)
FcNP	245 (4.89), 317 (4.49), 388 (3.82), 473 (3.68)
$FcNP_2$	234 (4.59), 314(4.29), 390 (3.68), 503 (3.11)
1	247(4.67), 361(4.83), 604(4.22)
2	248 (3.81), 317(3.37), 384(3.12), 467 (2.75)
3	241 (5.45), 316 (5.30), 384(4.77), 474(4.56), 594 (2.17)
4	240 (5.00), 320(4.75), 362(4.68), 597 (3.85)
5	237 (5.00), 327 (5.06), 466(2.11)
6	248 (3.46), 345(3.32), 590(2.43)

spectra display high energy bands below 250 nm which are assigned to $\pi \rightarrow \pi^*$ transitions localized on the Cp-NP units.[32] Low energy absorptions are attributed to the ferrocene based spin-allowed d−d transition and Fe(d) → Cp-NP(π^*) metal-to-ligand charge-transfer (MLCT) transitions. Protonation at the NP unit lowers the energy of Fe-centered highest occupied molecular orbital (HOMO) by withdrawing electron density away from the metal as evidenced by the increase in oxidation potential (see Table 1). The low-lying Cp-NP π^* orbitals are stabilized upon protonation resulting in red-shifting of the MLCT transitions. Further, increased mixing of the metal orbitals with appropriate Cp-NP orbitals enhances the MLCT character of a transition and thus causes an increase in the absorption intensity.[33] Figure 7 compares the absorption

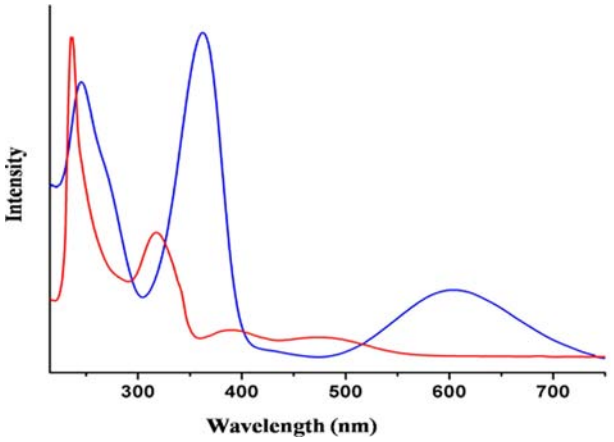

Figure 7. Electronic absorption spectra for FcNP (red line) and **1** (blue line) in dichloromethane at room temperature.

spectra of FcNP and its protonated complex **1**. On protonation, the d-d and MLCT bands of FcNP are significantly red-shifted accompanied by increase in molar absorption coefficient values (Table 2). Protonated FcNP units are characterized by a low-energy (~600 nm) broad MLCT band as observed in complexes **1**, **3**, **4**, and **6**.

Further on the Structure of 6. The association of two positively charged protonated $FcNP_2$ in **6** is intriguing. Since the positions of hydrogens could not be ascertained accurately from X-ray diffraction, we carried out density functional theory (DFT) calculations. The optimized structure of the dimer $[(FcNP_2{\cdot}H)^+]_2$ (B97D/6-311++G(d,p) (C,H,N)/LANL2DZ (Fe)) closely resembles the X-ray geometry. Use of a functional incorporating dispersion correction (B97D)[34] afforded planar arrangement of the NP rings in the dimer (Figure 8). This is in contrast to the twisted nonplanar configuration of the NP rings at the B3LYP level of calculation (Supporting Information, Figure S3). It is apparent that dispersive forces are critical to reproduce the X-ray geometry for the protonated dimer. The protons are nearly equidistant from the nitrogens (H1···N3/N4 = 1.269/1.264 Å). Careful examinations revealed that two protons are not exactly on top of each other alleviating the unfavorable repulsion. The H1 makes a shorter contact with N6 (2.899 Å) than H2 (3.196 Å). The same is true for H2 (H2···N3 = 2.899 Å). Other than the in-plane N···H contacts, the perpendicular H···N interactions play a role in overcoming the Coulombic repulsion between two protonated $FcNP_2$. Intramolecular π(NP)−π(NP) (3.592(1) Å) and intermolecular π(Cp)−π(NP) (3.638(3)Å) interactions (Supporting Information, Figure S4) are the key driving forces for the stacked head-on dimer in the solid-state.

Complex **6** is sufficiently soluble in common organic solvent which allowed for spectroscopic analysis. All protons in $FcNP_2$ and its protonated form **6** are unambiguously assigned by ^1H NMR (Supporting Information, Figures S5, S6) and ^1H−^1H COSY (Supporting Information, Figure S7, S8) spectroscopy.

dx.doi.org/10.1021/ic302155e | Inorg. Chem. 2013, 52, 1432−1442

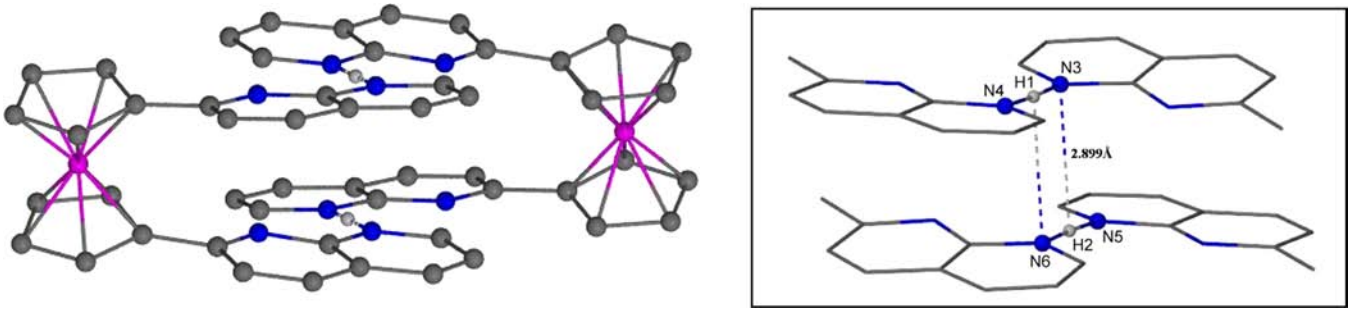

Figure 8. DFT optimized (B97D/LANL2DZ/6-311++G(d,p)) geometry for $[(FcNP_2{\cdot}H)_2]^{2+}$ (left). Illustration of the in-plane and perpendicular N···H interactions (right).

$FcNP_2$ exhibits five sets of nonequivalent NP protons and two sets of Cp protons (Supporting Information, Table S1). Protonated $FcNP_2$ exhibits a similar pattern in CD_3CN; however, all protons are downfield shifted due to protonation.

The X-ray structure of **6** reveals short separations (2.170(1), 2.467(1) Å) between H_a and H_{α}' (of the second molecule) because of the head-on dimer formation (Supporting Information, Figure S9). We performed NOE experiments to gain insight into solution structure. An intensity enhancement for H_b as well as H_{α}' is expected for the dimer structure on irradiation of H_a. Similarly, enhancements for H_{β}, H_e, and H_a' protons are expected for irradiation at H_{α}. The absence of any change in the intensity for H_{α} and H_a while irradiating H_a and H_{α}, respectively, is not in agreement with a close approach of two protonated $FcNP_2$ in solution (Supporting Information, Figures S10–S12). An intramolecular H-bonded structure for the protonated Fc*Py_2 (1,1′-bis(2-pyridyl)-octamethylferrocene)[35] prompted us to look for an analogous structure of $[FcNP_2.H]^+$ monomer. Half of the $[FcNP_2{\cdot}H]_2^{2+}$ dimer was subjected to DFT optimization which afforded a chelate structure engaging proton in between two inclined NP units (Supporting Information, Figure S13). The calculated N2···N3 distance is 2.509 Å, N2/N3···H distance of 1.283 Å, and the inclination angles of the NP rings from Cp planes are ~35°. An alternate protonated $FcNP_2$ monomer with hydrogen bridging between proximal nitrogens (N1) could not be optimized. Invariably it gave back the N8 protonated structure. The dimer was computed to be stable ($\Delta G = -7.63$ kcal/mol) compared to the monomer questioning the existence of the later in solution (see Supporting Information, Table S2).[36]

Proposed Mechanism. We monitored the protonation/demetalation reactions of FcNP by NMR spectroscopy. All acids employed in this work afford protonated products at first as evidenced by ^1H NMR spectra. For example, the NMR spectrum of 1:1 FcNP/HPic in CD_3OD shows sharp signals corresponding to protonated FcNP. The signals start broadening after around 6 h which suggests demetalation of FcNP releasing free Fe^{II} in the solution. The same observations were made for other acids except for HBF_4 for which only protonated FcNP was observed even after 12 h. The protonated salts are isolated for HBF_4 and CF_3SO_3H. Although all acids caused demetalation barring HBF_4, Fe complexes are successfully isolated for CF_3COOH, HCl, and HPic. NMR study reveals Fe extrusion for CF_3SO_3H, but an analytically pure compound could not be obtained.

The "free" iron in compounds **2**–**5** is the result of acid-mediated demetalation of FcNP. We offer a tentative mechanism for the Fe extrusion. The reaction proceeds with an initial protonation of the NP nitrogen as evidenced by the isolation of the protonated salts. The NP protonation drains the electron density of the Cp ring toward the NP unit thereby weakening the Fe-Cp interactions. The conjugate base attacks the electrophilic Fe in $[FcNP.H]^+$ facilitating the release of Cp rings from the metal eventually causing metal extrusion.

We made an effort to establish a quantitative correlation between demetalated organic product Cp-NP and "extruded-Fe". A careful experiment involving FcNP and picric acid (HPic) in methanol and subsequent treatment with KOH allowed the isolation of Cp-NP.[37] A slightly higher amount of Cp-NP was isolated with respect to $Fe(FcNP)(Pic)_2$ (1.18:1). Ideally this value should be 1:1. We attribute this discrepancy to an incomplete isolation of Fe complex by crystallization.

The $FcNP_2$ does not undergo demetalation under identical conditions. Two NP units share one positive charge, and hence weaken the Fe-Cp interaction to an extent that is not sufficient for demetalation. Acid mediated demetalation has been observed only for the monosubstituted ferrocene and not from the disubstituted ferrocene unit in a bis-ferrocenyl-azaheterocycle.[16]

Concluding Remarks. Reactions of protonic acids with ferrocene-naphthyridine hybrids FcNP and $FcNP_2$ are described in this work. All acids employed in this work afford protonated FcNP initially. Corresponding salts are isolated for HBF_4 or CF_3SO_3H. Longer reaction time leads to partial metal extrusion for each acid except for HBF_4. The (protonated) FcNP and the conjugate base trap the released Fe affording isolable complexes. Two different products **2** and **3** are isolated when FcNP and CF_3COOH are employed in 1:1 and 1:10 molar ratio, respectively. Only **4** is isolated with HCl irrespective of the amounts of acid used. Use of excess picric acid did not afford a clean product whereas **5** was isolated for 1:1 FcNP and acid. Metal extrusion was also observed for CF_3SO_3H from NMR study but an analytically pure compound could not be isolated. All complexes reported in this work are charge-neutral except the simple protonated salts. Longer reaction time (10–12 h) appears to be essential for demetalation. The acid-mediated demetalation proceeds with an initial protonation of the NP nitrogen. Subsequently, the conjugate base attacks the electrophilic Fe facilitating the metal extrusion. The conjugate base plays an important role in the demetalation process and in the isolation of Fe complex as well.

The $FcNP_2$ does not undergo demetalation under identical conditions. Two NP units share one positive charge and hence weaken the Fe-Cp interaction to a lesser extent not sufficient for demetalation. X-ray structure of the monoprotonated $FcNP_2$ reveals a discrete dimer $[(FcNP_2{\cdot}H)]_2[OTf]_2$ (**6**) supported by two N–H···N hydrogen bonds. Crystal packing and dispersive forces associated with the intra- and

dx.doi.org/10.1021/ic302155e | Inorg. Chem. 2013, 52, 1432–1442

Table 3. Crystallographic Data and Pertinent Refinement Parameters for Compounds 1−7

	1	2	3	4	5	6	7
empirical formula	$C_{19}H_{15}F_3FeN_2O_3S$	$C_{40}H_{32}F_6Fe_3N_4O_6$	$C_{52}H_{34}F_{24}Fe_5N_4O_{18}$	$C_{54}H_{45}C_{19}Fe_5N_6$	$C_{48}H_{32}Cl_2Fe_4N_{10}O_{14}$	$C_{27}H_{19}F_3FeN_4O_3S$	$C_{56}H_{40}F_{12}Fe_2N_8O_{12}S_4$
formula weight	464.24	946.25	1738.08	1376.26	1267.14	592.37	1484.90
crystal system	monoclinic	monoclinic	monoclinic	triclinic	triclinic	triclinic	triclinic
space group	$P2_1/c$	$P2_1/n$	$P2_1/n$	$P\bar{1}$	$P\bar{1}$	$P\bar{1}$	$P\bar{1}$
a (Å)	17.0369(7)	10.8588(8)	10.8059(10)	10.5470(9)	10.0600(10)	9.0818(10)	10.205(3)
b (Å)	11.8732(5)	9.2461(7)	20.0299(19)	17.1793(15)	10.2769(11)	11.8202(14)	13.222(4)
c (Å)	20.1878(9)	18.2394(14)	14.4707(14)	17.3383(15)	12.5815(13)	12.4100(14)	22.065(6)
α (deg)	90.00	90.00	90.00	60.4130(10)	98.906(2)	117.740(2)	82.369(5)
β (deg)	114.7910(10)	95.4850(10)	103.468(2)	89.053(2)	106.418(2)	98.255(2)	87.672(5)
γ (deg)	90.00	90.00	90.00	88.380(2)	101.995(2)	93.425(2)	75.108(5)
V (Å3)	3707.3(3)	1822.9(2)	3045.9(5)	2730.8(4)	1188.4(2)	1154.6(2)	2851.7(13)
Z	8	2	2	2	1	2	2
ρ_{calcd} (g cm^{-3})	1.664	1.724	1.895	1.674	1.771	1.704	1.729
μ (mm^{-1})	0.980	1.265	1.311	1.781	1.392	0.810	0.767
F(000)	1888	960	1728	1388	640	604	1504
reflections							
collected	32932	15862	15219	24954	10714	5863	25629
independent	9155	4437	5150	13191	5641	3866	13617
observed [$I > 2\sigma(I)$]	6668	3393	4478	6842	3987	3400	8270
no. of variables	531	276	474	679	352	372	847
GOF	1.057	1.094	0.980	0.939	1.026	1.046	1.060
R_{int}	0.0422		0.0276	0.0401	0.0341	0.0186	0.0541
final R indices	R1 = 0.0440	R1 = 0.0403	R1 = 0.0372	R1 = 0.0466	R1 = 0.0509	R1 = 0.0368	R1 = 0.0668
[$I > 2\sigma(I)$][a]	wR2 = 0.1042	wR2 = 0.0639	wR2 = 0.0888	wR2 = 0.0933	wR2 = 0.1085	wR2 = 0.0933	wR2 = 0.1449
R indices (all data)[a]	R1 = 0.0671	R1 = 0.0926	R1 = 0.0441	R1 = 0.1119	R1 = 0.0804	R1 = 0.0430	R1 = 0.1179
	wR2 = 0.1212	wR2 = 0.1055	wR2 = 0.0927	wR2 = 0.1201	wR2 = 0.1265	wR2 = 0.0972	wR2 = 0.1911

[a] $R_1 = \sum||F_o| - |F_c||/\sum|F_o|$ with $F_o^2 > 2\sigma(F_o^2)$. $wR_2 = [\sum w(|F_o^2| - |F_c^2|)^2/\sum|F_o^2|^2]^{1/2}$.

dx.doi.org/10.1021/ic302155e | Inorg. Chem. 2013, 52, 1432−1442

intermolecular $\pi-\pi$ stacking interactions (NP···NP and Cp···NP) allow the formation of the stacked dimer in the solid-state.

EXPERIMENTAL SECTION

General Procedures and Materials. All reactions were carried out under an inert nitrogen atmosphere with the use of standard Schlenk-line techniques. Solvents were dried by conventional methods, distilled under nitrogen, and deoxygenated prior to use. FcNP and $FcNP_2$ were prepared by following literature procedures.[38]

Physical Measurements. Elemental analyses were carried out using a Thermoquest CE instruments model EA/110 CHNS-O elemental analyzer. ESI-MS spectra were recorded on a Waters Micromass Quattro Micro triple-quadrupole mass spectrometer. The ^{1}H NMR spectra were obtained on a JEOL JNM-LAMBDA 500 MHz spectrophotometer. ^{1}H NMR chemical shifts were referenced to the residual hydrogen signal of the deuterated solvents. Infrared spectra were recorded on a Bruker Vertex 70 FTIR spectrophotometer in the ranges from 400 to 4000 cm^{-1} using KBr pellets. UV−visible spectra were recorded using a Jasco V-670 UV/vis absorption spectrophotometer. Cyclic voltammetric studies were performed on a BAS Epsilon electrochemical workstation in propylene carbonate with 0.1 M tetra-*n*-butylammonium hexafluorophosphate($TBAPF_6$) as the supporting electrolyte. The working electrode was a BAS Pt disk electrode. The reference electrode was Ag/AgCl, and the auxiliary electrode was a Pt wire. The ferrocene/ferrocenium couple occurs at $E_{1/2}$= +0.47 (60) V versus Ag/AgCl under the same experimental conditions. The potentials are reported in volts; the ΔE ($E_{p,a} - E_{p,c}$) values are in millivolts at a scan rate of 100 mV s^{-1}.

X-ray Data Collection and Refinement. . Single-crystal X-ray studies were performed on a CCD Bruker SMART APEX diffractometer equipped with an Oxford Instruments low-temperature attachment. All data were collected at 100(2) K using graphite monochromated Mo K_α radiation (λ_α) 0.71073 (Å). The frames were indexed, integrated, and scaled using the SMART and SAINT software packages,[39] and the data were corrected for absorption using the SADABS programs.[40] Structures were solved and refined with the SHELX suite of programs[41] as implemented in X-Seed,[42] while additional crystallographic calculations were performed by the program PLATON.[43] The figures were drawn using ORTEP.[44] CCDC nos. 872201−872207 contain the supplementary crystallographic data for compounds **1**−**7**. These data can be obtained free of charge from the Cambridge Crystallographic Data Centre via www.ccdc.cam.ac.uk/data_request/cif. The N−H hydrogens and water hydrogens were located in a difference Fourier map. The remaining hydrogen atoms were included at geometrically calculated positions in the final stages of the refinement and were refined according to the "riding model". All non-hydrogen atoms were refined with anisotropic thermal parameters unless mentioned otherwise. Pertinent crystallographic data for compounds **1**−**7** are summarized in Table 3.

Computational Details. Full geometry optimization calculations were performed at the DFT/B97D level of theory.[33] Calculations were carried out by means of the G09 package.[45] The double-ζ basis set of Hay and Wadt (LanL2DZ) with effective core potential (ECP) was used for Fe.[46] The remaining atoms (H, C, and N) were described using 6-311++G(d,p) basis sets.[47]

Syntheses. ***Caution!*** *Picrate salts are potentially explosive. Only small amounts of compound were synthesized and handled with extreme care under dark condition and low temperature.*

Synthesis of [FcNP·H][OTf] (1). To a methanolic solution (15 mL) of FcNP (150 mg, 0.48 mmol) was added a 0.5 mL 1(M) methanolic solution of HOTf (0.5 mmol) dropwise with stirring. The mixture immediately turned purple. After stirring for 1 h at room temperature, the resulting purple solution was concentrated to a small volume under vacuum, and 15 mL of diethyl ether was added with stirring to induce precipitation. The solid residue was then filtered and washed with diethyl ether (3 × 10 mL). Finally, it was dried under vacuum to afford **1**. Yield: 184 mg (83%). X-ray-quality crystals were grown by layering petroleum ether onto a dichloromethane solution of **1** inside an 8 mm o.d. vacuum-sealed glass tube. Anal. Calcd for $C_{19}H_{15}N_2Fe_1F_3SO_3$: C, 49.16; H, 3.26; N, 6.03. Found: C, 49.28; H, 3.21; N, 6.12. IR (KBr, cm^{-1}): ν (FcNP) 1627(s), 1572(s), 1504(s), 1436(m), 1384(s), 1290 (w), 836 (m), 496 (m); ν (OTf^-) 1240(vs), ν (NH) 3095 (br, m). ^{1}H NMR (CD_3CN, δ): 8.94 (s, br, H_a), 8.76 (s, br, H_c), 8.49 (s, br, H_d), 7.84 (s, br, $H_{e,b}$), 5.46(s, br, H_α), 5.05(s, br, H_β), 4.33 (s, br, H_{cp}). ESI-MS: m/z 315 $[M]^+$.

Synthesis of $[Fe(O_2CCF_3)_2(FcNP)_2(H_2O)_2]$ (2). To a methanolic solution (15 mL) of FcNP (94 mg, 0.3 mmol) was added a 0.3 mL 1(M) methanolic solution of trifluoroacetic acid (0.3 mmol), and the mixture was stirred for 12 h at room temperature. The resulting purple solution was concentrated under vacuum, and 15 mL of diethyl ether was added with stirring to induce precipitation. The red solid residue was filtered, washed with diethyl ether (3 × 10 mL), and dried under vacuum to afford **2**. Yield: 60 mg (63%). X-ray-quality crystals were grown by layering petroleum ether onto a dichloromethane solution of **2** inside an 8 mm o.d. vacuum-sealed glass tube. Anal. Calcd for $C_{40}H_{32}F_6Fe_3N_4O_6$: C, 50.77; H, 3.41; N, 5.92. Found: C, 50.53; H, 3.52; N, 6.02. IR (KBr, cm^{-1}): ν (FcNP) 1610(s), 1555(s), 1511(s), 1443(m), 1383(w), 918 (m), 837 (m), 783 (w); ν (CF_3CO_2) 1664(vs), 1202(s), 1180(vs); ν (H_2O), 3429(m).

Synthesis of $[Fe_3(OH_2)_2(O_2CCF_3)_8(FcNP{\cdot}H)_2]$ (3). The reaction of FcNP (90 mg, 0.29 mmol) and 1(M) methanolic solution of trifluoroacetic acid (3 mL, 3 mmol) was carried out for 12 h following a procedure similar to that described for the synthesis of **2**. Yield: 70 mg (70%). Single crystals were grown by the diffusion of petroleum ether onto a dichloromethane solution of **3** inside an 8 mm o.d. vacuum-sealed glass tube. Anal. Calcd for $C_{52}H_{34}N_4O_{18}F_{24}Fe_5$: C, 35.93; H, 1.97; N, 3.22. Found: C, 36.02; H, 1.88; N, 3.27. FT-IR (KBr, cm^{-1}): ν (FcNP) 1613(m), 1561(m), 1510(m), 1445(w), 1388(w), 718(w), 473(m); ν ($CF_3CO_2^-$) 1701(vs), 1204(vs), 1150(s); ν (H_2O) 3423(m); ν (NH) 3141 (m).

Synthesis of $[(FcNP{\cdot}H)_3(Cl)][FeCl_4]_2$ (4). The reaction of FcNP (85 mg, 0.27 mmol) and 1(M) HCl in Et_2O (0.4 mL, 0.4 mmol) was carried out for 12 h following a procedure similar to that described for the synthesis of **1**. Yield: 53 mg (72%). Single crystals were grown by the diffusion of petroleum ether onto a dichloromethane solution of the **4** inside an 8 mm o.d. vacuum-sealed glass tube. Anal. Calcd for $C_{54}H_{45}N_6Cl_9Fe_5$: C, 47.13; H, 3.30; N, 6.11. Found: C, 47.22; H, 3.18; N, 6.21. IR (KBr, cm^{-1}): ν (FcNP) 1618(m), 1556(m), 1512(m), 1443(w), 1390(w), 714(w), 471(m).

Synthesis of $[Fe_2(Cl)_2(FcNP)_2(Pic)_2]$ (5). To a methanolic solution (15 mL) of FcNP (100 mg, 0.32 mmol) was added a methanolic solution of picric acid (87 mg, 0.38 mmol), and the resulting dark green solution was stirred for 12 h at room temperature. The solution was then concentrated, and 15 mL of diethyl ether was added with stirring to induce precipitation. The resulting green solid residue was filtered and washed with diethyl ether (3 × 10 mL). Finally, it was dried in a desiccator with $CaCl_2$ as desiccant to afford **5**. Yield: 65 mg (64%). Single crystals were grown by diffusion of petroleum ether onto a dichloromethane solution of **5** inside an 8 mm o.d. vacuum-sealed glass tube. Anal. Calcd for $C_{48}H_{32}Cl_2Fe_4N_{10}O_{14}$: C, 45.50; H, 2.55; N, 11.05. Found: C, 45.37; H, 2.64; N, 11.13.

Synthesis of $[\{FcNP_2{\cdot}H\}_2\{CF_3SO_3\}_2]$ (6) and $[FcNP_2{\cdot}H_2][CF_3SO_3]_2$ (7). To a methanolic solution (15 mL) of $FcNP_2$ (124 mg, 0.28 mmol) was added a 0.3 mL 1(M) methanolic solution of triflic acid (0.3 mmol) with stirring. Immediately, the mixture turned blue, and the resulting blue solution was stirred for an hour at room temperature. Then the solution was concentrated, and 15 mL of diethyl ether was added with stirring to induce precipitation. The resulting blue solid residue was washed with diethyl ether (3 × 10 mL) and dried in a vacuum to afford a blue solid. Yield: 150 mg (90%). Single crystals of **6** were grown by the diffusion of petroleum ether onto a dichloromethane solution of the blue solid inside an 8 mm o.d. vacuum-sealed glass tube. Needle type crystals of **6** were collected, and the mother liquor was kept in a refrigerator. After 3 weeks, a few block shaped crystals of **7** were harvested. Yield: 8 mg (4%). For compound **6**: Anal. Calcd for $C_{27}H_{19}N_4F_3SO_3Fe_1$: C, 54.75; H, 3.23; N, 9.46. Found: C, 54.82; H, 3.28; N, 9.38. IR (KBr, cm^{-1}): ν (OTf^-) 1246 (vs), 1027(s); ν ($FcNP_2$) 1630 (m), 1611 (m), 1575 (m), 1505 (w),

dx.doi.org/10.1021/ic302155e | *Inorg. Chem.* 2013, 52, 1432−1442

1436 (m), 1387 (m), 843 (m); ν (N−H) 3085 (m). ^{1}H NMR (CD_3CN, δ): 8.84 (br,s, H_a), 8.65 (d, H_c, $J_{b,c}$ = 6.1 Hz), 8.15 (d, H_d, $J_{d,e}$ = 8 Hz), 7.84 (br,m, H_b), 7.65 (d, H_e, $J_{d,e}$ = 7.2 Hz), 5.29(s, H_α), 4.84 (s, H_β). ESI-MS: m/z 443 $[M]^+$. For compound **7**: Anal. Calcd for $C_{28}H_{20}N_4O_6S_2F_6Fe_1$: C, 45.30; H, 2.72; N, 7.55. Found: C, 45.12; H, 2.68; N, 7.49.

■ ASSOCIATED CONTENT

Supporting Information

ORTEP diagrams for **1** and **4**, NMR spectra for $FcNP_2$ and protonated $FcNP_2$, crystal packing diagram of **6**, optimized geometries, energies, atomic coordinates for $[(FcNP_2{\cdot}H)]^+$ and $\{(FcNP_2{\cdot}H)_2\}^{2+}$ are provided. This material is available free of charge via the Internet at http://pubs.acs.org.

■ AUTHOR INFORMATION

Corresponding Author

*Fax: +91-512-2597436. Tel: + 91-512-2597336. E-mail: jbera@iitk.ac.in.

Notes

The authors declare no competing financial interest.

■ ACKNOWLEDGMENTS

We thank an anonymous reviewer for insightful comments and suggestions. Helpful discussions with Prof. Shridhar R. Gadre on the computational work are greatly appreciated. This work is financially supported by the Department of Science and Technology (DST), India, and Council of Scientific and Industrial Research (CSIR), India. J.K.B. thanks DST for the Swarnajayanti fellowship. M.S. thanks CSIR and T.G thanks UGC, India, for fellowships.

■ DEDICATION

Dedicated to Professor R. N. Mukherjee on the occasion of his 60th birthday.

■ REFERENCES

(1) (a) Prakash, G. K. S.; Buchholz, H.; Reddy, V. P.; Meijere, A. de.; Olah, G. A. *J. Am. Chem. Soc.* **1992**, *114*, 1097. (b) Hop, C. E. C. A.; McMahon, T. B. *J. Am. Soc. Mass. Spectrom.* **1994**, *5*, 274. (c) Ikonomou, M. G.; Sunner, J.; Kebarle, P. *J. Phys. Chem.* **1988**, *92*, 6308. (d) Bühl, M.; Grigoleit, S. *Organometallics* **2005**, *24*, 1516. (e) Borisov, Y. A.; Ustynyuk, N. A. *Russ. Chem. Bull., Int.Ed.* **2002**, *51*, 1900. (f) Jungwirth, P.; Stussi, D.; Weber, J. *Chem. Phys. Lett.* **1992**, *190*, 29.

(2) Curphey, T. J.; Santer, J. O.; Rosenblum, M.; Richards, J. H. *J. Am. Chem. Soc.* **1960**, *82*, 5249.

(3) Meot, M.-N. *J. Am. Chem. Soc.* **1989**, *111*, 2830.

(4) (a) Cunningham, A. F., Jr. *J. Am. Chem. Soc.* **1991**, *113*, 4864. (b) Cunningham, A. F., Jr. *Organometallics* **1997**, *16*, 1114. (c) Mayor-López, M. J.; Weber, J.; Mannfors, B.; Cunningham, A. F., Jr. *Organometallics* **1998**, *17*, 4983.

(5) Mueller-Westerhoff, U. T.; Haas, T. J.; Swiegers, G. F.; Leipert, T. K. *J. Organomet. Chem.* **1994**, *472*, 229.

(6) McKee, M. L. *J. Am. Chem. Soc.* **1993**, *115*, 2818.

(7) Mayor-López, M. J.; Lüthi, H. P.; Koch, H.; Morgantini, P. Y.; Weber, J. *J. Chem. Phys.* **2000**, *113*, 8009.

(8) (a) Ilkhechi, A. H.; Mercero, J. M.; Silanes, I.; Bolte, M.; Scheibitz, M.; Lerner, H. W.; Ugalde, J. M.; Wagner, M. *J. Am. Chem. Soc.* **2005**, *127*, 10656. (b) Scheibitz, M.; Winter, R. F.; Bolte, M.; Lerner, H. W.; Wagner, M. *Angew. Chem., Int. Ed.* **2003**, *42*, 924. (c) Scholz, S.; Green, J. C.; Lerner, H. W.; Bolte, M.; Wagner, M. *Chem. Commun.* **2002**, 36.

(9) (a) Oton, F.; Espinosa, A.; Tarraga, A.; de Arellano, C. R.; Molina, P. *Chem.—Eur. J.* **2007**, *13*, 5742. (b) Alfonso, M.; Espinosa, A.; Tarraga, A.; Molina, P. *Chem. Commun.* **2012**, *48*, 6848.

(10) (a) Neshvad, G.; Roberts, R. M. G.; Silver, J. *J. Organomet. Chem.* **1982**, *236*, 349. (b) Olah, G. A.; Mo, Y. K. *J. Organomet. Chem.* **1973**, *60*, 311.

(11) Šarić, A.; Vrček, V.; Bühl, M. *Organometallics* **2008**, *27*, 394.

(12) (a) Togni, A., Hayashi, T., Eds.; *Ferrocenes*; VCH Publishers: Weinheim, Germany, 1995. (b) Braga, D.; Polito, M.; Bracaccini, M.; D'Addario, D.; Tagliavini, E.; Proserpio, D. M.; Grepioni, F. *Chem. Commun.* **2002**, 1080. (c) Chen-jie, F.; Chun-ying, D.; Dong, G.; Cheng, H.; Qing-jin, M.; Zheming, W.; Chun-hua, Y. *Chem. Commun.* **2001**, 2540. (d) Horikoshi, R.; Nambu, C.; Mochida, T. *Inorg. Chem.* **2003**, *42*, 6868. (e) Zhu, Y.; Wolf, M. O. *J. Am. Chem. Soc.* **2000**, *122*, 10121. (f) Gao, Y.; Twamley, B.; Shreeve, J. M. *Organometallics* **2006**, *25*, 3364. (g) Reger, D. L.; Brown, K. J.; Gardinier, J. R.; Smith, M. D. *Organometallics* **2003**, *22*, 4973. (h) Guo, S. L.; Peters, F.; Fabrizi de Biani, F.; Bats, J. W.; Herdtweck, E.; Zanello, P.; Wagner, M. *Inorg. Chem.* **2001**, *40*, 4928. (i) Caballero, A.; Lloveras, V.; Curiel, D.; Tàrraga, A.; Espinosa, A.; Garcia, R.; Vidal-Gancedo, J.; Rovira, C.; Wurst, K.; Molina, P.; Veciana, J. *Inorg. Chem.* **2007**, *46*, 825. (j) Ion, A.; Moutet, J.-C.; Saint-Amam, E.; Royal, G.; Tingry, S.; Pecaut, J.; Menage, S.; Ziessel, R. *Inorg. Chem.* **2001**, *40*, 3632. (k) Buda, M.; Moutet, J.-C.; Saint-Aman, E.; Cian, A. D.; Fischer, J.; Ziessel, R. *Inorg. Chem.* **1998**, *37*, 4146. (l) Siemeling, U.; Brüggen, J. V. D.; Vorfeld, U.; Neumann, B.; Stammler, A.; Stamler, H.-G.; Brockhinke, A.; Plessow, R.; Zanello, P.; Laschi, F.; Biani, F. F. D.; Fontani, M.; Steenken, S.; Stapper, M.; Gurzadyn, G. *Chem.—Eur. J.* **2003**, *9*, 2819. (m) Dong, T.-Y.; Chen, K.; Lin, M.-C.; Lee, L. *Organometallics* **2005**, *24*, 4198. (n) Irigoras, A.; Mercero, J. M.; Silanes, I.; Ugalde, J. M. *J. Am. Chem. Soc.* **2001**, *123*, 5040. (o) Zapata, F.; Caballero, A.; Espinosa, A.; Tárraga, A.; Molina, P. *Inorg. Chem.* **2009**, *48*, 11566. (p) Otón, F.; Ratera, I.; Espinosa, A.; Wurtz, K.; Parella, T.; Tárraga, A.; Veciana, J.; Molina, P. *Chem.—Eur. J.* **2010**, *16*, 1532. (q) Singh, N.; Kumar, A.; Prasad, R.; Molloy, K. C.; Mahon, M. F. *Dalton Trans.* **2010**, *39*, 2667. (r) Zapata, F.; Caballero, A.; Espinosa, A.; Tárraga, A.; Molina, P. *Dalton Trans.* **2009**, 3900. (s) Wei, K.; Ni, J.; Liu, Y. *Inorg. Chem.* **2010**, *49*, 1834. (t) Weiss, M.; Frey, W.; Peters, R. *Organometallics* **2012**, *31*, 6365. (u) Yuan, P.; Liu, S. H.; Xiong, W.; Yin, J.; Yu, G.; Sung, H. Y.; Williams, I. D.; Jia, G. *Organometallics* **2005**, *24*, 1452.

(13) (a) Takemoto, S.; Kuwata, S.; Nishibayashi, Y.; Hidai, M. *Inorg. Chem.* **1998**, *37*, 6428. (b) Ramos, A.; Otten, E.; Stephan, D. W. *J. Am. Chem. Soc.* **2009**, *131*, 15610. (c) Metallinos, C.; Tremblay, D.; Barrett, F. B.; Taylor, N. J. *J. Organomet. Chem.* **2006**, *691*, 2044. (d) Cui, X. L.; Delgado, R.; Costa, J.; Drew, M. G. B.; Costa, P. J.; Felix, V. *Polyhedron* **2010**, *29*, 1697. (e) Otón, F.; Espinosa, A.; Tárraga, A.; Molina, P. *Organometallics* **2007**, *26*, 6234. (f) Enders, M.; Kohl, G.; Pritzkow, H. *Organometallics* **2002**, *21*, 1111.

(14) Enders, M.; Ludwig, G.; Pritzkow, H. *Organometallics* **2002**, *21*, 3856.

(15) Trifan, D. S.; Nicholas, L. *J. Am. Chem. Soc.* **1957**, *79*, 2746.

(16) (a) Lopez, J. L.; Tárraga, A.; Espinosa, A.; Velasco, M. D.; Molina, P.; Lloveras, V.; Gancedo, J. V.; Rovira, C.; Veciana, J.; Evans, D. J.; Wurst, K. *Chem.—Eur. J.* **2004**, *10*, 1815. (b) Tárraga, A.; Molina, P.; López, J. L.; Espinosa, A. D.; Evans, J. *Tetrahedron Lett.* **2002**, *43*, 4717.

(17) (a) Sadhukhan, N.; Bera, J. K. *Inorg. Chem.* **2009**, *48*, 978. (b) Sadhukhan, N.; Patra, S. K.; Sana, K.; Bera, J. K. *Organometallics* **2006**, *25*, 2914.

(18) Patra, S. K.; Rahaman, S. M. W.; Majumdar, M.; Sinha, A.; Bera, J. K. *Chem. Commun.* **2008**, 2511.

(19) (a) Tshuva, E. Y.; Lippard, S. J. *Chem. Rev.* **2004**, *104*, 987. (b) Solomon, E. I.; Brunold, T. C.; Davis, M. I.; Kemsley, J. N.; Lee, S.-K.; Lehnert, N.; Neese, F.; Skulan, A. J.; Yang, Y.-S.; Zhou, J. *Chem. Rev.* **2000**, *100*, 235. (c) Kurtz, D. M., Jr. *Chem. Rev.* **1990**, *90*, 585. (d) Wallar, B. J.; Lipscomb, J. D. *Chem. Rev.* **1996**, *96*, 2625. (e) Du Bois, J.; Mizoguchi, T. J.; Lippard, S. J. *Coord. Chem. Rev.* **2000**, *200–202*, 443.

(20) Whittington, D. A.; Lippard, S. J. *J. Am. Chem. Soc.* **2001**, *123*, 827.
(21) (a) Gherman, B. F.; Dunietz, B. D.; Whittington, D. A.; Lippard, S. J.; Friesner, R. A. *J. Am. Chem. Soc.* **2001**, *123*, 3836. (b) Gherman, B. F.; Baik, M. H.; Lippard, S. J.; Friesner, R. A. *J. Am. Chem. Soc.* **2004**, *126*, 2978.
(22) (a) Hagen, K. S.; Lachicotte, R. *J. Am. Chem. Soc.* **1992**, *114*, 8741. (b) Hagen, K. S.; Lachicotte, R.; Kitaygorodskiy, A.; Elbouadili, A. *Angew. Chem., Int. Ed. Engl.* **1993**, *32*, 1321. (c) Coucouvanis, D.; Reynolds, R. A., III; Dunham, W. R. *J. Am. Chem. Soc.* **1995**, *117*, 7550. (d) Yoon, S.; Kelly, A. E.; Lippard, S. J. *Polyhedron* **2004**, *23*, 2805. (e) Yoon, S.; Lippard, S. J. *J. Am. Chem. Soc.* **2004**, *126*, 16692. (f) Feng, S. *Acta Crystallogr.* **2008**, *E64*, m817. (g) Hagen, K. S.; Lachicotte, R.; Kitaygorodskiy, A. *J. Am. Chem. Soc.* **1993**, *115*, 12617.
(23) (a) Rabe, V.; Frey, W.; Baro, A.; Laschat, S.; Bauer, M.; Bertagnolli, H.; Rajagopalan, S.; Asthalter, T.; Roduner, E.; Dilger, H.; Glaser, T.; Schnieders, D. *Eur. J. Inorg. Chem.* **2009**, 4660. (b) Bond, A. M.; Clark, R. J. H.; Humphrey, D. G.; Panayiotopoulos, P.; Skelton, B. W.; White, A. H. *J. Chem. Soc., Dalton Trans.* **1998**, 1845. (c) Tolis, E. I.; Helliwell, M.; Langley, S.; Raftery, J.; Winpenny, R. E. P. *Angew. Chem., Int. Ed.* **2003**, *42*, 3804. (d) Keeney, L.; Hynes, M. J. *Dalton Trans.* **2005**, 1524. (e) Pandey, A. K.; Gupta, T.; Baranwal, B. P. *Transition Met. Chem.* **2004**, *29*, 370. (f) Zhang, K. L.; Shi, Y. J.; Gao, S.; Dai, Y. D.; Yu, K. B.; You, X. Z. *Inorg. Chem. Commun.* **2004**, *7*, 584. (g) Cooper, P.; Tuna, F.; Shanmugam, M.; Sorace, L.; Heath, S. L.; Collison, D.; McInnes, E. J. L.; Winpenny, R. E. P. *Inorg. Chim. Acta* **2008**, *361*, 3663. (h) Murugesu, M.; Abboud, K. A.; Christou, G. *Polyhedron* **2004**, *23*, 2779. (i) Boudalis, A. K.; Donnadieu, B.; Nastopoulos, V.; Clemente-Juan, J. M.; Mari, A.; Sanakis, Y.; Tuchagues, J. P.; Perlepes, S. P. *Angew. Chem., Int. Ed.* **2004**, *43*, 2266. (j) Cannon, R. D.; White, R. P. *Prog. Inorg. Chem.* **1988**, *36*, 195.
(24) Rardin, L.; Bino, A.; Poganiuch, P.; Toman, W. B.; Liu, S.; Lippard, J. *Angew. Chem., Int. Ed. Engl.* **1990**, *29*, 812.
(25) $Fe(FcNP)(Pic)_2$: Yield: 47%. Anal. Calcd for $C_{30}H_{18}N_8O_{14}Fe_2$: C, 43.61; H, 2.20; N, 13.56. Found: C, 44.37; H, 2.44; N, 13.13. IR (KBr, cm^{-1}): ν (NO_2) 1635 (vs), 1612 (vs), 1562 (vs), 1511 (s), ν (FcNP) 1495 (m), 1430 (m), 1374(m), 1343(m), 1284 (m). CV (propylene carbonate, Volt): 0.61 (120) ($E_{1/2}$), 0.11 ($E_{p,a}$), −1.87 ($E_{p,c}$). UV−vis (CH_3CN, nm): 322 (3.76), 375 (5.11), 495 (1.98). ESI-MS (CH_3OH): m/z 629 for $[Fe(FcNP)(Pic)(CH_3OH)]^+$.
(26) Bera, J. K.; Sadhukhan, N.; Majumdar, M. *Eur. J. Inorg. Chem.* **2009**, 4023.
(27) (a) Beer, P. D.; Drew, M. G. B.; Grieve, A.; Ogden, M. I. *J. Chem. Soc., Dalton Trans.* **1995**, 3455. (b) Ayala, J. D.; Zinner, L. B.; Vicentini, G.; Pra, A. D.; Bombieri, G. *Inorg. Chim. Acta* **1993**, *211*, 161. (c) Fernandes, L. C.; Matos, J. R.; Zinner, L. B.; Vicentini, G.; Zukerman-Schpector, J. *Polyhedron* **2000**, *19*, 2313. (d) Fan, L.; Liu, W.; Gan, X.; Tang, N.; Tan, M.; Jiang, W.; Yu, K. *Polyhedron* **2000**, *19*, 779. (e) Guo, Y. L.; Dou, W.; Wang, Y. W.; Sheng, W.; Wang, D. Q. *Polyhedron* **2007**, *26*, 1699.
(28) (a) Liu, Z. Q.; Li, Y. T.; Wu, Z. Y.; Song, Y. L. *Inorg. Chim. Acta* **2008**, *361*, 226. (b) Song, Y. L.; Li, Y. T.; Wu, Z. Y.; Zhang, G. L.; Sun, F. *Acta Crystallogr., Sect. E: Struct. Rep. Online* **2006**, *62*, m2558. (c) Dong, W. K.; Feng, J. H.; Wang, L.; Xu, L.; Zhao, L.; Yang, X. Q.; Yu, T. Z. *Transition Met. Chem.* **2007**, *32*, 1101. (d) Seo, J.; Song, M. R.; Sultana, K. F.; Kim, H. J.; Kim, J.; Lee, S. S. *J. Mol. Struct.* **2007**, *827*, 201. (e) Song, M. R.; Lee, J. E.; Lee, S. Y.; Seo, J.; Park, K. M.; Lee, S. S. *Inorg. Chem. Commun.* **2006**, *9*, 75. (f) Bibal, B.; Tinant, B.; Declercq, J. P.; Dutasta, J. P. *Chem. Commun.* **2002**, 432. (g) Harrowfield, J. M.; Sharma, R. P.; Skelton, B. W.; White, A. H. *Aust. J. Chem.* **1998**, *51*, 735. (h) Galesic, N.; Herceg, H.; Sevdic, D. *Acta Crystallogr., Sect. C: Cryst. Struct. Commun.* **1987**, *13*, 1135.
(29) (a) Wang, Y. W.; Guo, Y. L.; Liu, W. S.; Yu, K. B. *Acta Crystallogr., Sect. E: Struct. Rep. Online* **2004**, *60*, m1801. (b) Wang, Y. W.; Guo, Y. L.; Liu, W. S.; Wang, D. Q. *Anal. Sci.: X-Ray Struct. Anal. Online* **2004**, *20*, x165. (c) Andrianov, V. G.; Struchkov, Y. T.; Pyshnograeva, N. I.; Setkina, V. N.; Kursanov, D. N. *J. Organomet. Chem.* **1981**, *206*, 177.
(30) Wang, X.-B.; Dai, B.; Woo, H.-K.; Wang, L.-S. *Angew. Chem., Int. Ed.* **2005**, *44*, 6022.
(31) Paolucci, D.; Marcaccio, M.; Bruno, C.; Braga, D.; Polito, M.; Paolucci, F. *Organometallics* **2005**, *24*, 1198.
(32) Yamaguchi, Y.; Ding, W.; Sanderson, C. T.; Borden, M. L.; Morgan, M. J.; Kutal, C. *Coord. Chem. Rev.* **2007**, *251*, 515.
(33) Carr, J. D.; Coles, S. J.; Hassan, W. W.; Hursthouse, M. B.; Malik, K. M. A.; Tucker, J. H. R. *J. Chem. Soc., Dalton Trans.* **1999**, 57.
(34) Grimme, S. *J. Comput. Chem.* **2006**, *27*, 1787.
(35) Moisan, L.; Borgne, T. L.; Thuéry, P.; Ephritikhine, M. *Acta Crystallogr., Sect C: Cryst. Struct. Commun.* **2002**, *C58*, m98.
(36) Geometry optimizations of both monomer and dimer forms of $[FcNP_2{\cdot}H]^+$ were carried out at different levels of theory (see, Supporting Information, Table S2). At B97D/6-311++G(d,p)/LANL2DZ (CPCM), the ΔG[dimer − 2× monomer] was computed to be −7.63 (−42.27) kcal/mol. This value is considerably lower (−2.23 kcal/mol) at the WB97XD level.
(37) A mixture of FcNP (50 mg, 0.16 mmol) and picric acid (44 mg, 0.19 mmol) was stirred vigorously in methanol for 12 h at room temperature. The solution was then concentrated, and 15 mL of diethyl ether was added with stirring to induce precipitation. The resulting solid was redissolved in 5 mL of acetonitrile and was layered with diethyl ether. After 5 days, red crystalline product $Fe(FcNP)(Pic)_2$ was isolated. The mother liquor was digested with methanolic KOH for 30 min. The solvent was then removed to obtain a solid residue. Cp-NP was purified by column chromatography using alumina as stationary phase and ethyl acetate/petroleum ether as eluent, and was identified by mass spectra. The molar ratio of Cp-NP and $Fe(FcNP)(Pic)_2$ was estimated to be 1.18:1.
(38) Gelin, F.; Thummel, R. P. *J. Org. Chem.* **1992**, *57*, 3780.
(39) *SAINT+ Software for CCD diffractometers*; Bruker AXS: Madison, WI, 2000.
(40) Sheldrick, G. M. *SADABS Program for Correction of Area Detector Data*; University of Göttingen: Göttingen, Germany, 1999.
(41) (a) *SHELXTL Package v. 6.10*; Bruker AXS: Madison, WI, 2000. (b) Sheldrick, G. M. *SHELXS-86 and SHELXL-97*; University of Göttingen: Göttingen, Germany, 1997.
(42) (a) Atwood, J. L.; Barbour, L. J. *Cryst. Growth Des.* **2003**, *3*, 3. (b) Barbour, L. J. *J. Supramol. Chem.* **2001**, *1*, 189.
(43) Spek, L. *PLATON*; University of Utrecht: Utrecht, The Netherlands, 2001.
(44) Farrugia, L. J. *J. Appl. Crystallogr.* **1997**, *30*, 565.
(45) Frisch, M. J.; Trucks, G. W.; Schlegel, H. B.; Scuseria, G. E.; Robb, M. A.; Cheeseman, J. R.; Montgomery, J. A., Jr.; Vreven, T.; Kudin, K. N.; Burant, J. C.; Millam, J. M.; Iyengar, S. S.; Tomasi, J.; Barone, V.; Mennucci, B.; Cossi, M.; Scalmani, G.; Rega, N.; Petersson, G. A.; Nakatsuji, H.; Hada, M.; Ehara, M.; Toyota, K.; Fukuda, R.; Hasegawa, J.; Ishida, M.; Nakajima, T.; Honda, Y.; Kitao, O.; Nakai, H.; Klene, M.; Li, X.; Knox, J. E.; Hratchian, H. P.; Cross, J. B.; Adamo, C.; Jaramillo, J.; Gomperts, R.; Stratmann, R. E.; Yazyev, O.; Austin, A. J.; Cammi, R.; Pomelli, C.; Ochterski, J. W.; Ayala, P. Y.; Morokuma, K.; Voth, G. A.; Salvador, P.; Dannenberg, J. J.; Zakrzewski, V. G.; Dapprich, S.; Daniels, A. D.; Strain, M. C.; Farkas, O.; Malick, D. K.; Rabuck, A. D.; Raghavachari, K.; Foresman, J. B.; Ortiz, J. V.; Cui, Q.; Baboul, A. G.; Clifford, S.; Cioslowski, J.; Stefanov, B. B.; Liu, G.; Liashenko, A.; Piskorz, P.; Komaromi, I.; Martin, R. L.; Fox, D. J.; Keith, T.; Al-Laham, M. A.; Peng, C. Y.; Nanayakkara, A.; Challacombe, M.; Gill, P. M. W.; Johnson, B.; Chen, W.; Wong, M. W.; Gonzalez, C.; Pople, J. A. *Gaussian 09*; Gaussian Inc.: Wallingford, CT, 2009.
(46) (a) Hay, P. J.; Wadt, W. R. *J. Chem. Phys.* **1985**, *82*, 270. (b) Wadt, W. R.; Hay, P. J. *J. Chem. Phys.* **1985**, *82*, 284. (c) Hay, P. J.; Wadt, W. R. *J. Chem. Phys.* **1985**, *82*, 299.
(47) (a) Binkley, J. S.; Pople, J. A.; Hehre, W. J. *J. Am. Chem. Soc.* **1980**, *102*, 939. (b) Hehre, W. J.; Ditchfield, R.; Pople, J. A. *J. Chem. Phys.* **1972**, *56*, 2257.